Journal of Parapsychology
2020, Vol. 84, No. 2, 254-275

http://doi.org/10.30891/jopar.2020.02.07

A Portable Bench for Research on Telekinetic Effects on a Spinning Mobile and Experimental Results Obtained with it [1]

Eric Dullin and David Jamet

Psychophysics and Cognitive Dissonance Laboratory

Abstract. In this paper we analyze precisely the starting conditions of the motion of a spinning target with the focus on the thermic/aerodynamic effects. We conducted reference experiments with a static bench, where the motion of the target is obtained with the airflow issuing from a pump, and PKer (volunteer practicing Psychokinesis) experiments (with a new portable bench), where the motion of the target inside the bench is triggered by the PKer. The comparison between the airflow speeds around the target in the two sets of experiments showed that the tangential airflow speeds in the PKer experiments were 10 times lower than the required tangential airflow speeds to start the target moving in the reference experiments. The potential bias and errors in the measurement and computation are shown to be minimal compared to the factor given above. Some particular experimental set-up, simulating the hand and the upper body of the PKer in proximity to the portable bench, did not provoke any reaction on the target. These different elements tend to prove that the motion of the target in these experiments cannot be attributed to thermal/aerodynamic effects. The portable bench could be a good way for other labs to try to reproduce and confirm these experiments.
Keywords: telekinesis; psychokinesis; airflow measurement; PIV portable bench; macro-pk;

In a conference held within a PA convention (Dullin & Jamet, 2017b), and a paper published in the Journal of Scientific Exploration (Dullin & Jamet, 2018), we presented research on historical perspectives concerning the study of psychokinesis on lightweight spinning objects, and a methodology for conducting macro-pk tests on this kind of target, in a non-confined environment.

After eliminating causes like magnetism, electrostatic forces, vibration, and radiation, the only causes remaining were aerodynamic forces (natural air currents or thermally generated air currents).

The approach to identifying the influence of these forces was to evaluate the ratio of spinning object rotational speed to object periphery airflow speed and the evolution of this ratio along the experiment (which may last several minutes).With this ratio, it was shown for a specific object (a plastic dome called Hemispheric Mobile (HM)) that pure aerodynamic effects (ratio lower than one) could be

1 Address correspondence to: Eric Dullin, Ph. D, Psychophysics and Cognitive Dissonance Laboratory (LAPDC), 13 allée jean Monnet, 86760, Neuville-de-Poitou, France, ericdullin@gmail.com. The authors wish to thank the University of West Georgia and Loy Auerbach for their contributions to archive research on the Martin Caidin case, as well as Karl Dries for his major contribution on all PKer experiments.

distinguished from other effects (motor-driven or potential macro-pk effect) with ratios significantly bigger than one (from two to seven).

We are in this paper presenting another way to analyze the phenomenon: determine through reference experiments at which threshold airflow speed the target starts to move, then analyze the airflow speeds during the start of experiments with PKer and see if they are corresponding to this threshold.

As it was presented in Dullin and Jamet, (2018), this kind of evaluation could not be found in the literature, mainly because of the lack of tools to evaluate slow airflow.

To improve the signal-to-noise ratio in experiments with PKers, and also to facilitate the use of this methodology by other labs or individuals, we developed a portable semi-confined bench. We will present here, in detail, the way it works and the improvement it brings to the global approach.

This bench requires an experiment PKer in order to produce effects (gifted participant).

We follow the idea to work with a non-confined or semi-confined environment using a partial physical isolation of the target system, with a measurement system ensuring control of the remaining known effect. As mentioned in Dullin and Jamet (2018), in Jahn and Dunne (2011) is presented the idea that uncertainty, using fewer constraints, could be a prerequisite for seeing larger phenomena. We could also mention the speculation in Puthoff and Targ (1974) following the experiments done with the gifted participant Ingo Swann in order to try to influence at a distance a superconducting differential magnetometer: “the subject thus appear to act as a local negentropic source. If true, it may be more advantageous as a practical matter to work with extremely noisy systems, rather than with highly constrained or organized systems, in order to maximize possible effects due to the introduction of order”.

Following the presentation of Martin Caidin’s work in Dullin and Jamet (2018), we did some further research on this case, going through the William G. Roll archives in the University of Georgia. Unfortunately, there was no publication except the letter of Roll to Dr. Michael Glancey of the University of Florida (Roll, 1988), reporting his experiments with Martin Caidin (10 hours) assisted by a video tape specialist from West Georgia College and one assistant. This letter presented pretty impressive results (targets from 0.5 to 90g, action from a position outside the room, stop and change of direction).

This research and the experiments were conducted without external funding (no conflict of interest).

Method

Hemispherical mobile device (HM)

A plastic dome (hemispheric shape with a flat part on the top) has been chosen (Figure M1). The shape and the smooth surface limit the interaction between the airflows and the HM.

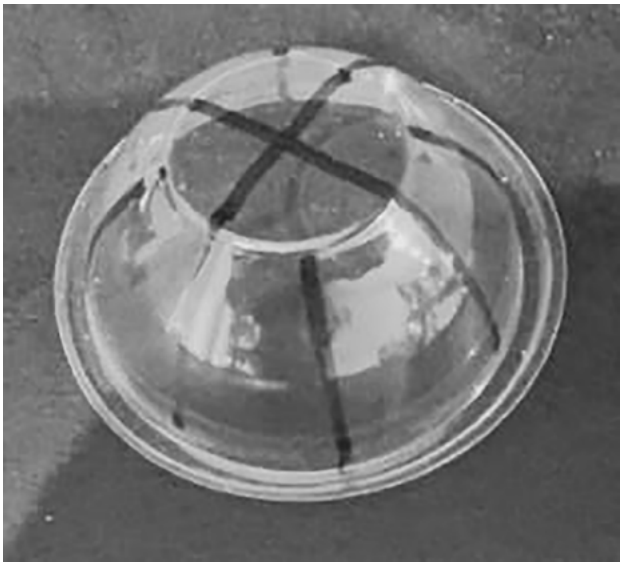

Figure M1. Hemispheric mobile (HM) device used for the experiments

The weight of the dome is 2.45 g, and its diameter is 85 mm. It is possible to find this kind of dome in retail shop : typically 4 oz (or approximately 125 ml) clear dome ice cream cup or plastic disposable round cup or clear plastic high dome lid for 4 oz. aluminum foil; the aluminum foil cupcake / ramekin could be used too although a bit more sensible to the airflows.

This dome is placed at the top of the stem of a carousel candle (Figure M2), also easily found in retail shops. The flat part on the top of the dome facilitates the balancing on the top of the carousel candle (as in these experiments we are not working with high speed, we don't need socket in order to maintain the dome in its position on the carousel candle rod).

Figure M2. HM installed on the stem from a carrousel candle

Airflow speeds measured by PIV

The core techniques used to evaluate the air currents' speed around the HM are described in detail in Dullin and Jamet (2018). They use the PIV (Particle Image Velocimetry) technique (Figure M3) in order to evaluate, with image processing, the speed of the smoke particles or/and smoke particle aggregates, driven by the air and illuminated by a laser beam. As the speed of the smoke/particles is induced by the speed of the air, it gives good information on the airflows moving around the HM.

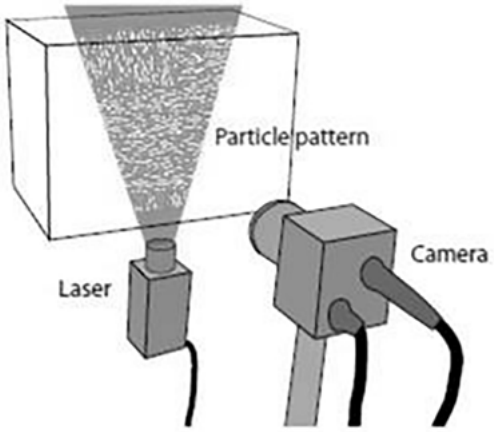

Figure M3. PIV set-up

Set-up for the reference experiments: airflow induction with pump

The first set-up for the reference experiment with a pump is the same as described in Dullin and Jamet (2018 and 2017b). It used a mechanism with a pump aspirating a mix of smoke and air. The output of the pump is pushed through a hose (such as one used in an aquarium), bringing the airflow to the PIV bench (Figure M4).

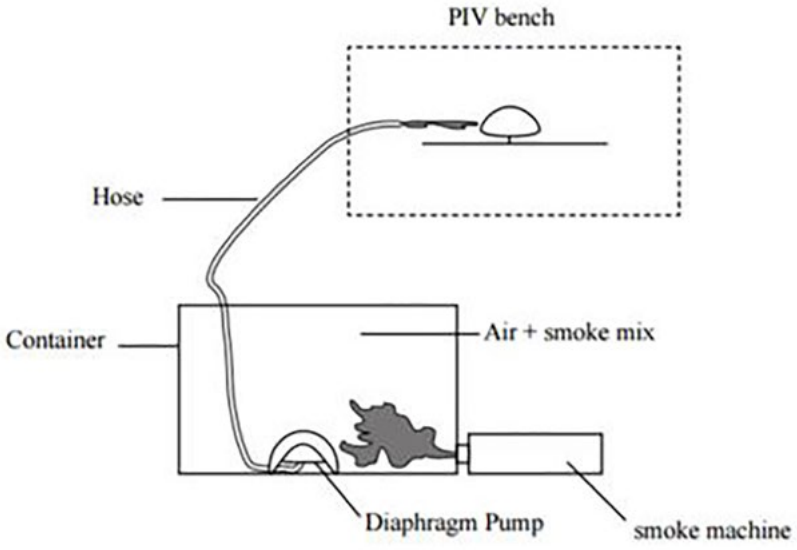

Figure M4. Mechanism for airflow generation in the reference experiment

In Figure M5, we can see the parts described above. The camera taking the images (50 images/s in a 1280 x 720 pixel resolution), is placed in a horizontal plane above, and parallel to the bench.

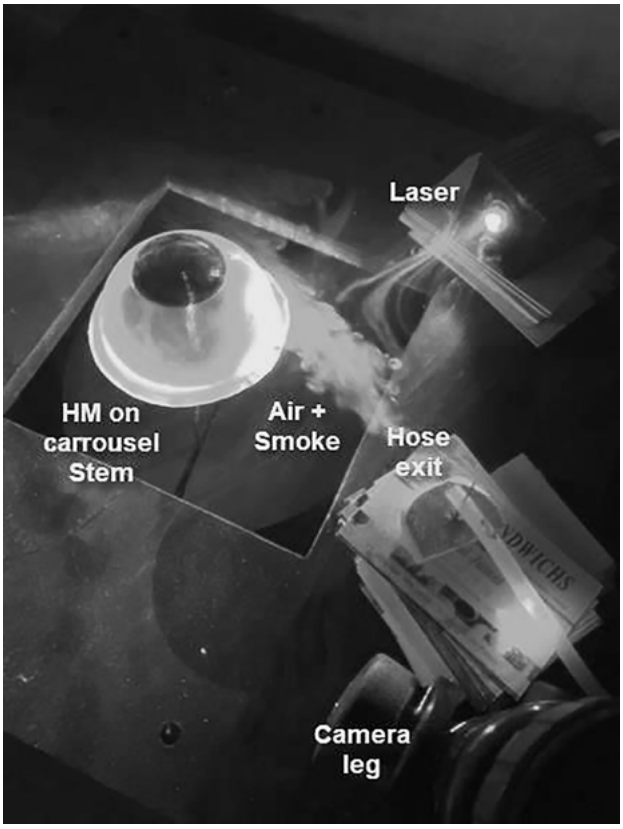

Figure M5. Airflow generation in the reference experiment

In order to facilitate other experimentation and also to open the experiments to other labs, a portable bench has been designed and constructed.

Experimental set-up for macro-Pk test: portable PIV bench

The reference experimental set-up is effective when the airflow is induced by a pump or a fan. But, when used with a PKer, the smoke generation can create noise in the experiment, which decreases the signal-to-noise ratio. Even though some good measurements were obtained with this bench (Dullin & Jamet, 2017b and c), we wanted to go a step further.

Also, we wanted to eliminate some other possible causes of the HM move as:

- The one proposed by Warcollier for the Tromelin's motor (Dullin & Jamet, 2017a and 2018)
- The one proposed by Nechayev and Perelman (Dullin & Jamet, 2017b and 2018)
- The one proposed by Albert Hofmann (Dullin & Jamet, 2018)

We also wanted a PKer to be able to work directly with a bench in a home environment, without having to come to the reference bench in a remote location. With that, we would be able to multiply the

experiments and also meet some good characteristics for the “mood” factor often presented as a key point in this kind of experiment. (Black & Carpenter, 2014).

So, a new bench has been developed with portable characteristics.

This bench (Figure M6) is constituted by:

- A plexiglass box with a lid. This lid has a rectangular opening in the middle (so we can work in a semi-confined environment)
- A support for the camera (30 image/s in a 1280 x 720 pixel resolution) to be placed above the opening
- One or two incense sticks placed in the box to generate smoke (thus, without any machinery, which works because of the semi-confined environment)
- A small laser device with a specific lens chosen to illuminate a thin horizontal or vertical air slice (visualized by the smoke).

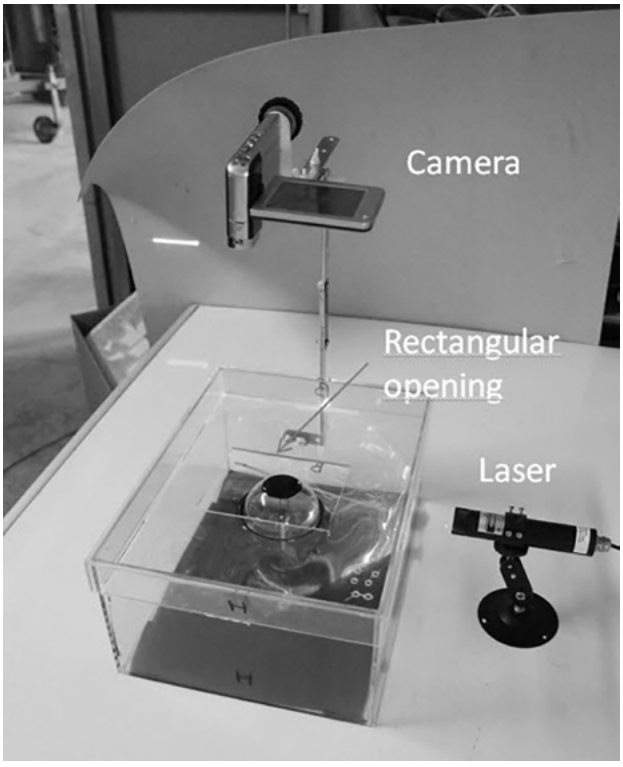

Figure M6. Portable PIV bench for macro-PK test

The way we operate the set-up is as follows:

- First, we place the target (HM plastic dome) on the carrousel stand inside the bench
- Then, we install the camera in order to see correctly the HM target in the field of view

- Then, we light the incense sticks
- After that, we turn on the laser and adjust its height so it illuminates the target at the right place. For horizontal PIV we set the horizontal plane around 1 cm above the HM base.
- Finally, we adjust the camera in order to have a sharp image of the target and the airflow.

With this experiment set-up, the PKer has to put his hand above the target, above or on the plexiglass box, and around the rectangular opening (Figure M7).

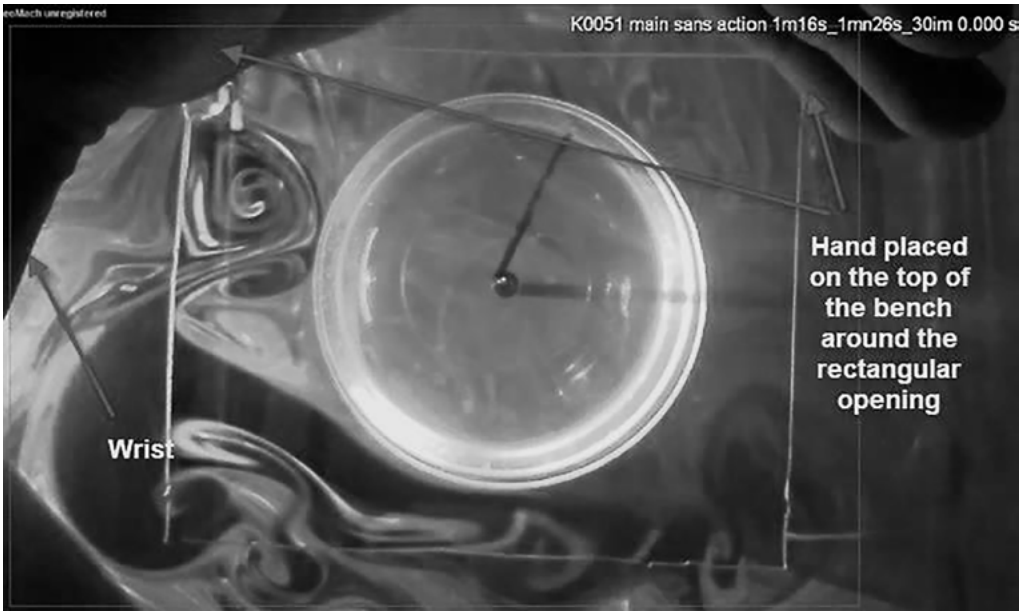

Figure M7. Portable PIV bench for macro-PK test: hand position

With this experimental configuration, the explanations of the target motion proposed by Warcollier, Nechayev and Hoffmann (Dullin & Jamet, 2018) do not apply, mainly because the hand is placed above the HM. Then, the hand cannot form an obstacle to air currents around the mobile (part of the Warcollier explanation).

Also, the temperature difference between the palm and the fingertips (Nechayev explanation of the target motion) can't influence the HM from above the plexiglass box. (See also the part of the Discussion section about the experiment studying the hand and upper body temperature effects.)

Finally, the wrist is far from the target, so it is difficult to imagine in this case that the pulse in the wrist (one of the Hoffmann's explanation of the target motion), which is already a very small effect, can induce a spinning motion of the HM (see also Dullin and Jamet (2018) on the vibration analysis).

The PKer succeeded to set the mobile in motion with this configuration in a semi-repeatable way. So, with him we have been able to conduct the experiments that follow.

Experiment protocol

In order to have the best signal-to-noise ratio possible, we worked with a heavier target. In fact, we stacked three HMs, which gave a weigh of 3 x 2.45 g = 7.35 g.

Contrary to the experiments described in Dullin and Jamet (2017b and 2018), where the focus was on comparing the target speed to the airflow speed, with the target already spinning, here we focused on the conditions of the start of the mobile.

So, experiments have been conducted to start the HM with an airflow issuing from a pump in the first set-up (Poitiers), and other experiments have been conducted with a PKer trying to start the mobile in the portable bench (Montpellier).

Then, the focus was to determine, in both cases, what were the airflow speeds around the target when it was starting to move.

As a way to compare between experiments, we selected for observation 10 seconds after the time when the target started to spin. For these 10 seconds, we evaluated for the airflow

- The different speeds of the smoke particles or aggregate around the HM represented by vectors (vector-field representation) for each frame (a frame is defined here as the difference between two sequential images)
- The mean of this speed vector field for the 10 seconds (so, for 500 frames in the reference experience and for 300 frames for the PKer experiments), which is represented in Figure M8.

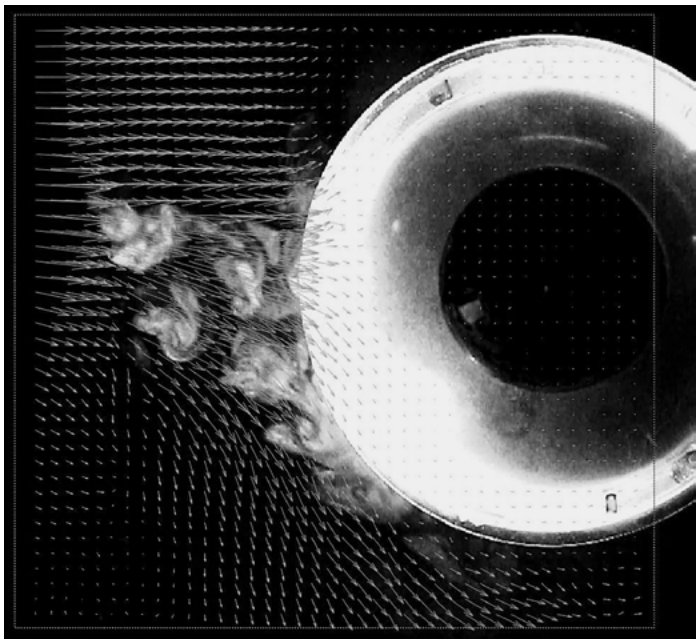

Figure M8. Mean speed vector field (with vector scale 8) for the selected 10 seconds

- The arrows represent the mean airflow speed at the considered point (base of the arrow) for the 10 seconds.

- The mean velocity magnitude of an area close to the HM and from where the movement could come. This gives information on the average value of the speed in this area regardless of the direction of each particle movement.

In Figure M9, for example, we have evaluated the mean velocity magnitude inside an area (the curved rectangle shape) close to the target, with a result of 34 mm/s.

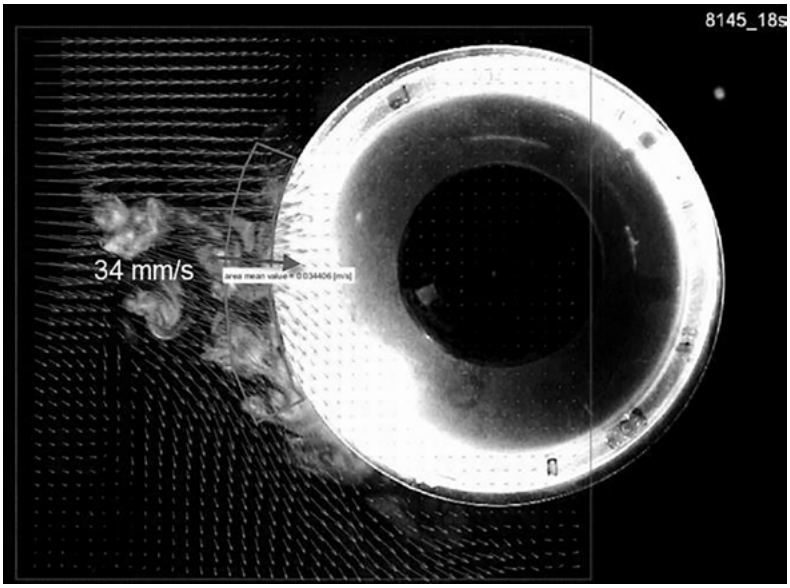

Figure M9. Area mean value for the velocity magnitude34 mm/s (vector scale 8)

In another step, we extract the components of the airflow speeds, tangential to 30 concentric circles around the target (Figure M10), as proposed in Dullin and Jamet (2018).

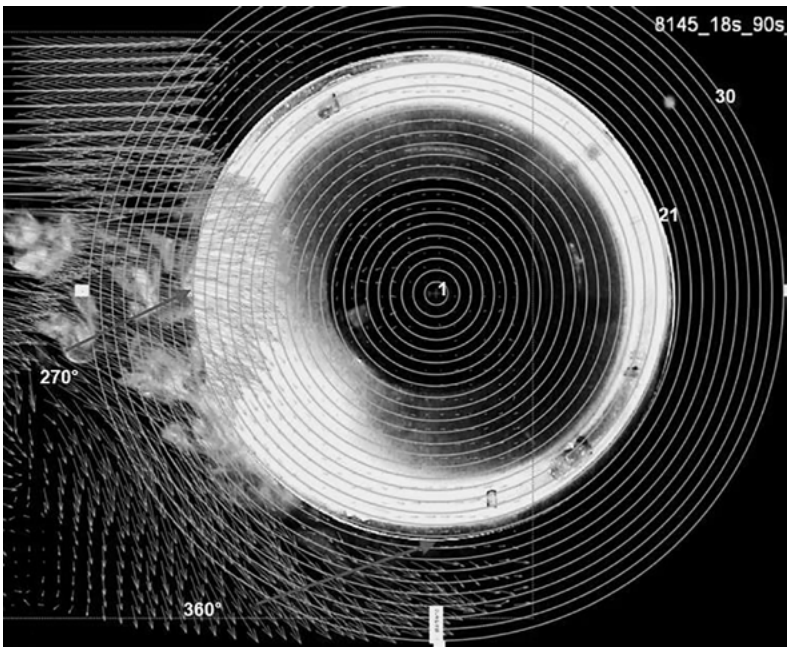

Figure M10. Concentric circles around the target for tangential speed extraction (vector scale 20)

Then we calculate a mean tangential speed for the different circles in the area impacted by the flow (270° to 360°, bottom-left quarter of the circles in the Figure M10). Finally, we draw the graph of these mean tangential speeds as a function of the circle number, which is presented in Figure M11. The outer circle is numbered “30”, and the circle at the periphery of the HM is numbered “21”.

This tangential speed is the component of the air speed which could drive the target by friction.

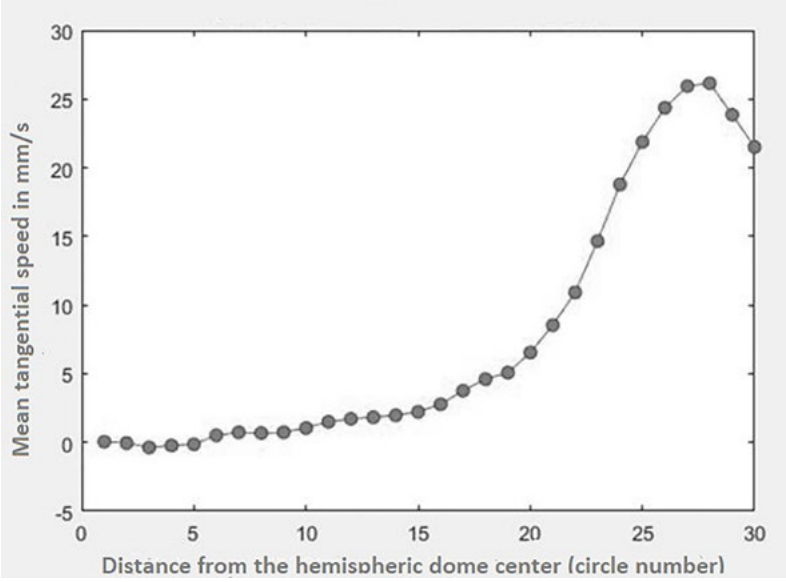

Figure M11. Mean tangential speed (in mm/s) as a function of the concentric circle concerned

For the presentation of the results and the comparison between experiments we will use this diagram, but with the use of the distance of the plastic dome surface in mm instead of the circle number.

Note: for the image treatment we use raw data, speed calculation, mean speed, and tangential speed without using any smoothing feature.

We also conducted for the PKer experiment

- An airflow speed analysis when the hand is in place on the top of the bench but without HM movement
- An airflow speed analysis when there is no hand in place (HM on the stem in the bench but no hand above the bench).

Trickery detection - other causes for movement

The techniques proposed (for airflow visualization) can easily detect any trickery involving aerodynamic forces used to move the HM (such as air blowing from the mouth—even if the PKer is wearing a mask—or hands moving).

Also, the way the HM is positioned in the bench makes it difficult to influence it from the outside of the bench to induce a spinning movement.

As the HM is made of plastic, the use of a magnet cannot induce a movement.

As presented in Dullin and Jamet (2018), static electricity could only induce some half-turn movement from one side to the other. Conversely, in the PKer experiments presented below, after the 10 second start, the PKer provoked a continuous run of the target of 4 minutes, finishing at a spin speed around 30 degrees/second before deciding to stop (Figure M12).

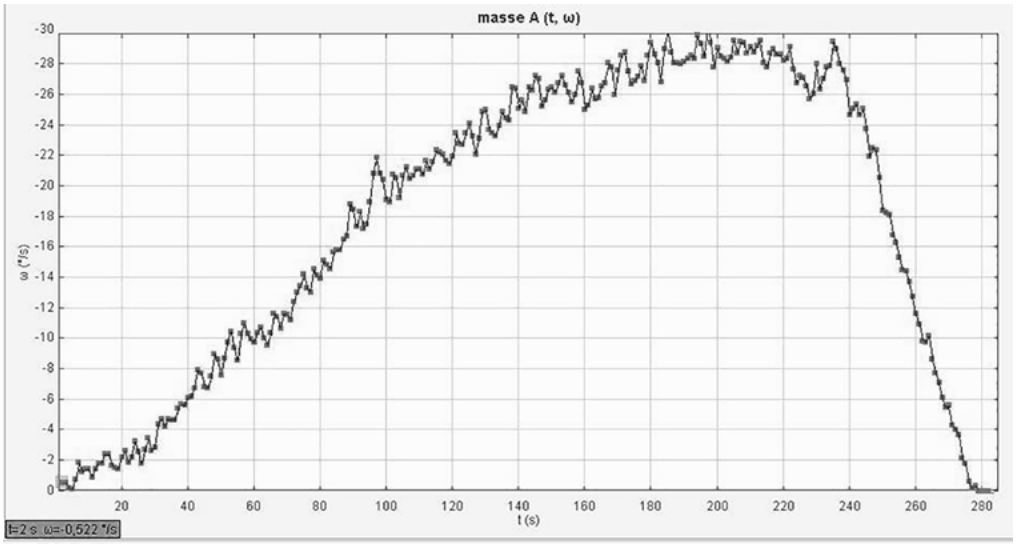

Figure M12. Spin speed evolution of the target (in degrees/second) as a function of time (in seconds), from motion start to stop, in the K0103 experiment (each experiment is attached to an internal reference number)

A-priori belief of the researchers

The three persons involved in these experiments were moderate to strong believers, before the project began, that these new experiments could show some results supporting the telekinesis hypothesis.

Results

Comparison of the speed vector fields between two reference experiments and two PKer experiments

To present the results, we will compare directly two reference ("pump") experiments with two PKer experiments.

Reminder: we conducted the "pump" experiments in such a way as to find the minimal speed of air required to start the target moving.

So, we conducted experiments adjusting the air speed and the hose exit orientation relative to the HM (Figure M5) in order to find this speed.

Then, as described in the Methods section, we go through a detailed study to evaluate the mean airflow speed around the target (which is clearly the cause of the motion in the reference experiment) and compare it with air speed in the PKer experiments.

So, first let us look at the four experiments using the mean speed vector fields during the 10 seconds when the target is starting to spin as a point of comparison (Figure R1).

The two upper images represent the reference experiments, one with a tangential air–smoke introduction (8162, on the left), the other (8145, on the right) a little bit more on the axis of the target.

Below them are images from the PKer experiments (K0103 and K0115).

The laser illuminated 0.5 centimeter above the base of the target in each case.

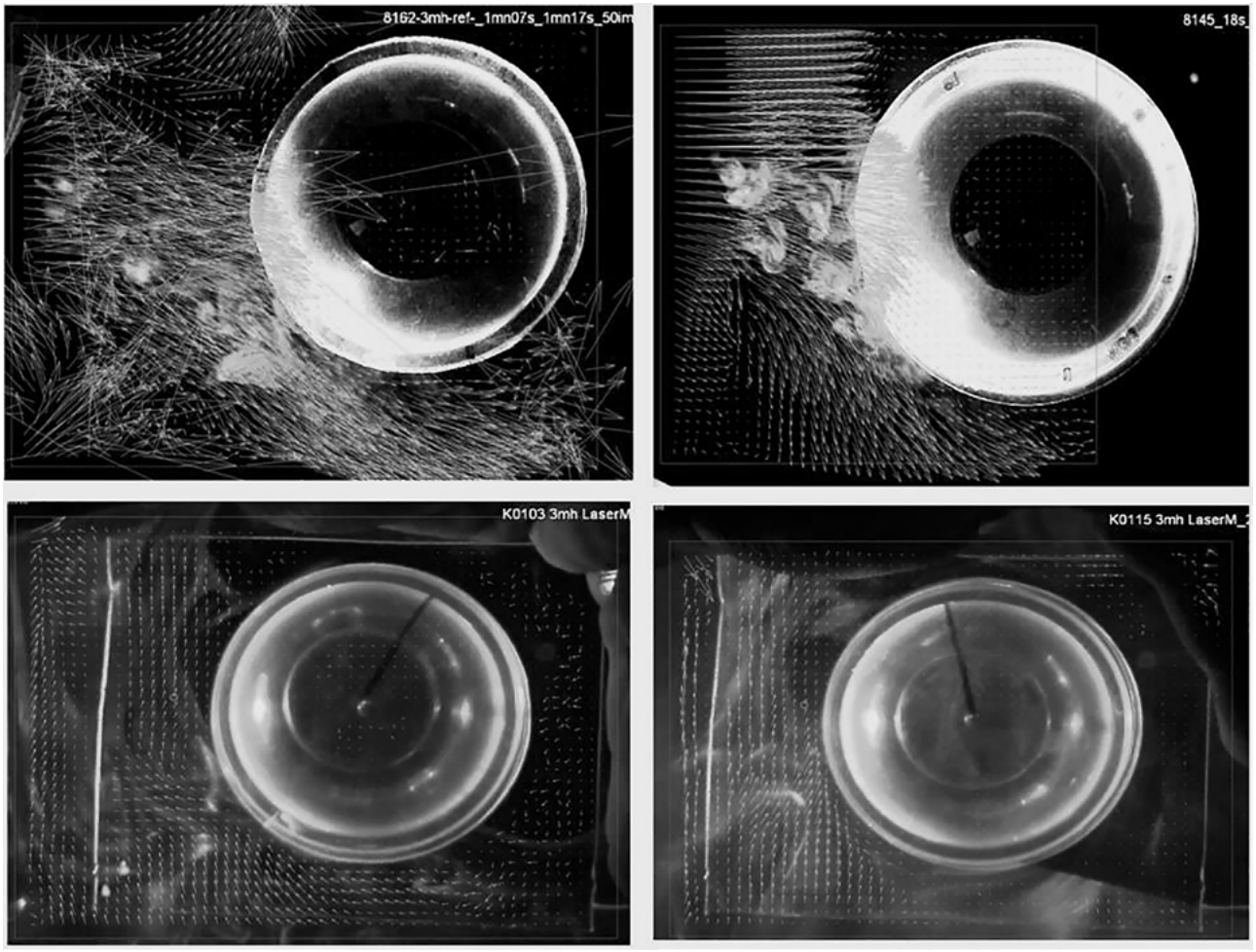

Figure R1. Speed vector field comparison between experiments 8162, 8145 (reference experiments, top two), and K0103, and K0115 (PKer experiments, bottom two)

As the speed vectors are at the same scale in all images (scale 20 in the PIV parameter), the difference between reference experiments and PKer experiments is quite evident at this stage.

Comparison of the velocity magnitude between two reference experiments and two PKer experiments

In evaluating the mean velocity magnitude in some areas around the HM where the airflow is correctly oriented to drive the HM, we obtained results shown in Figure R2.

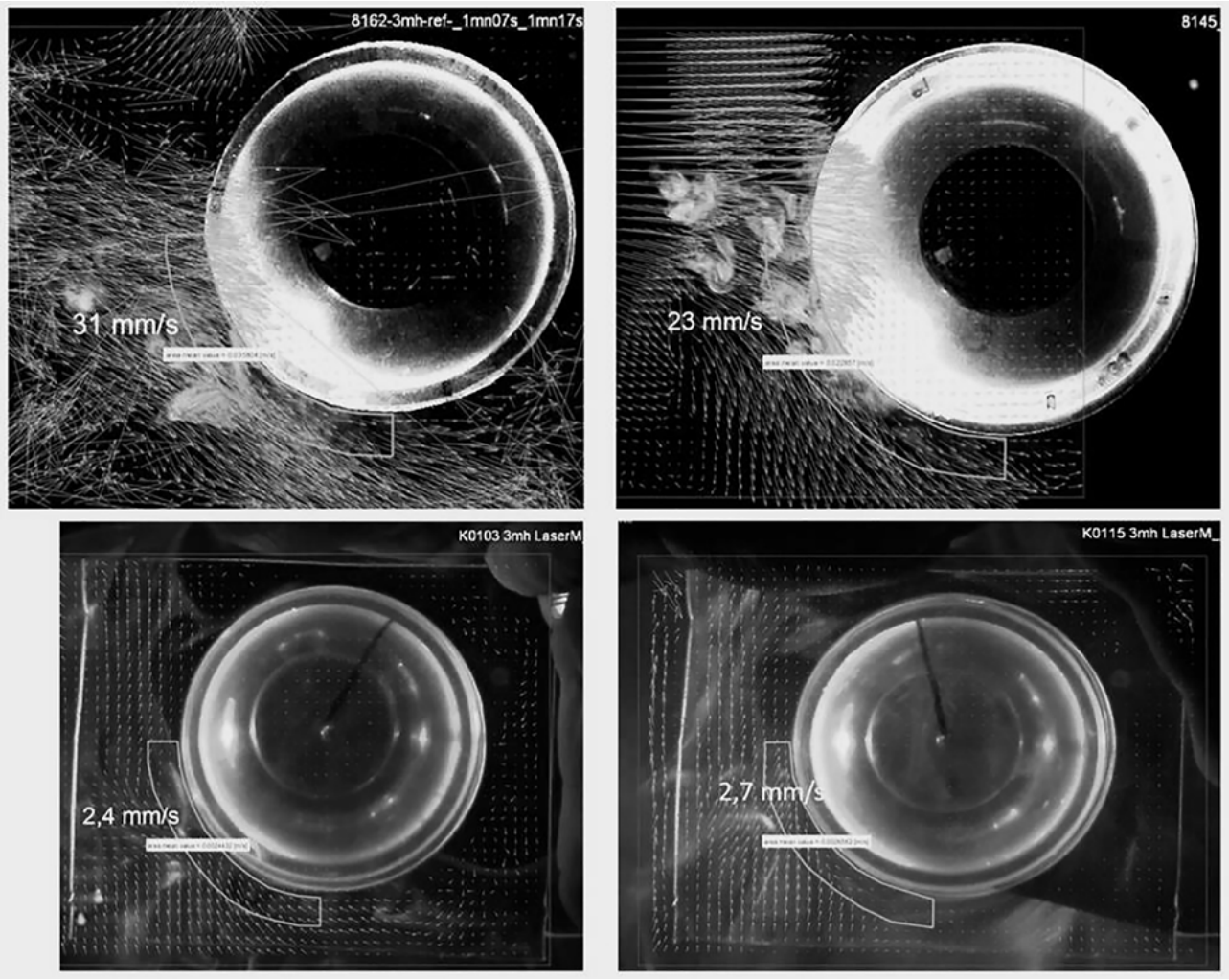

Figure R2. Mean velocity magnitude in areas close to the target
(Reference experiments, top two, PKer experiments, bottom two).

So, if we compare the lowest airflow velocity required to start the target moving with a pump (23 mm/s) with the mean speed measured when the HM starts to spin with a PKer (2.55 mm/s), we get a ratio of 9.

Comparison of the tangential airflow speed vectors between two reference experiments and two PKer experiments

In order to have a more accurate comparison, we computed the tangential speed in the different circles (see Methods section).

In Figure R3, the mean tangential speed in the angular section 270°–360°[2] is represented as a function of the radial distance from the surface of the HM for the four experiments.

Between 5 and 15 mm from the target surface, this diagram gives an average ratio of air speeds of 10 between the 8145 reference experiments and the PKer experiments and a ratio of 15 between the 8162 reference experiment and the PKer experiments. At 1 cm from the surface we have the following values for the airflow tangential speed:

- Reference experiment 8162: 29.4 mm/s
- Reference experiment 8145: 18.8 mm/s
- PKer experiment K0103: 1.5 mm/s
- PKer experiment K0115: 2.2 mm/s

This gives a ratio between the lowest tangential speed of reference to the mean of the speed in PKer experiments equal to 18.8/1.85 = 10.2.

Airflow speed comparison between experiments with PKer action and experiments with no action

It could be interesting to look at the airflow speed either when the PKer has his hand on the transportable bench, but no motion is induced on the target, or when there is no hand present, and no action from the PKer.

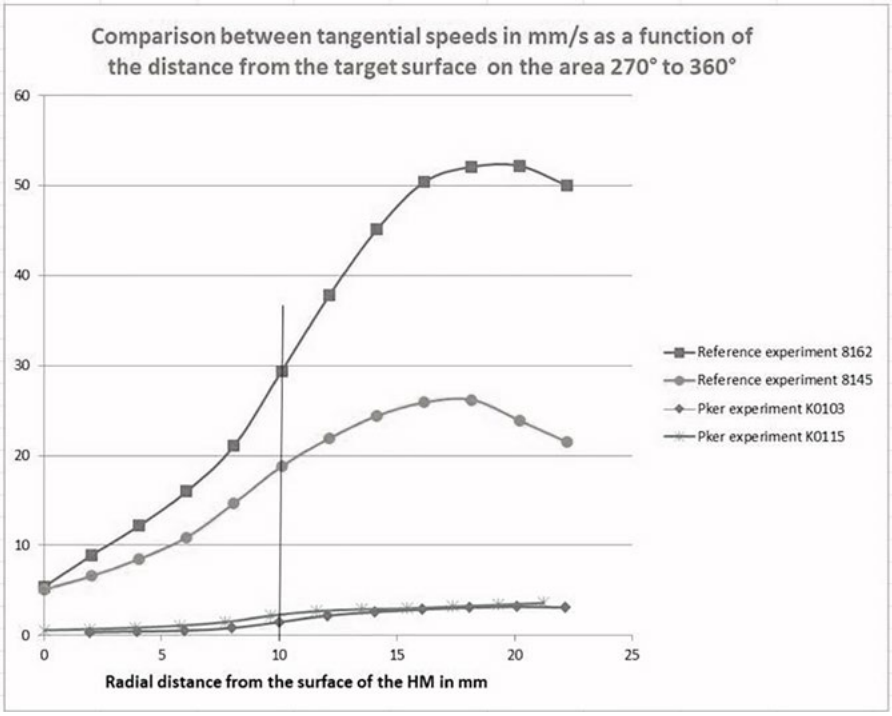

Figure R3. Tangential air speeds in mm/s as a function of the radial distance from the HM surface in mm

2 For more details, see the Discussion section "*Choice of impact zone for calculation*", below.

We conducted these experiments, which are presented in Figure R4,

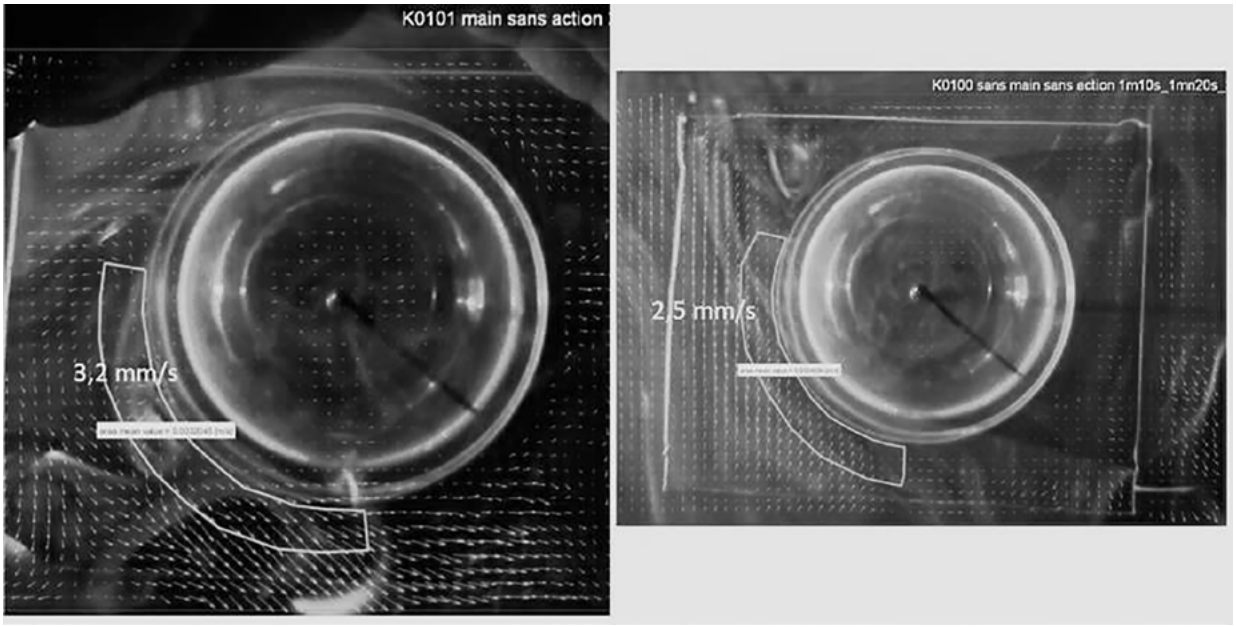

Figure R4. Left image: hand present without action. Right image: neither hand nor action

and in Figure R5 are the resulting curves compared to the two other PKer experiments.

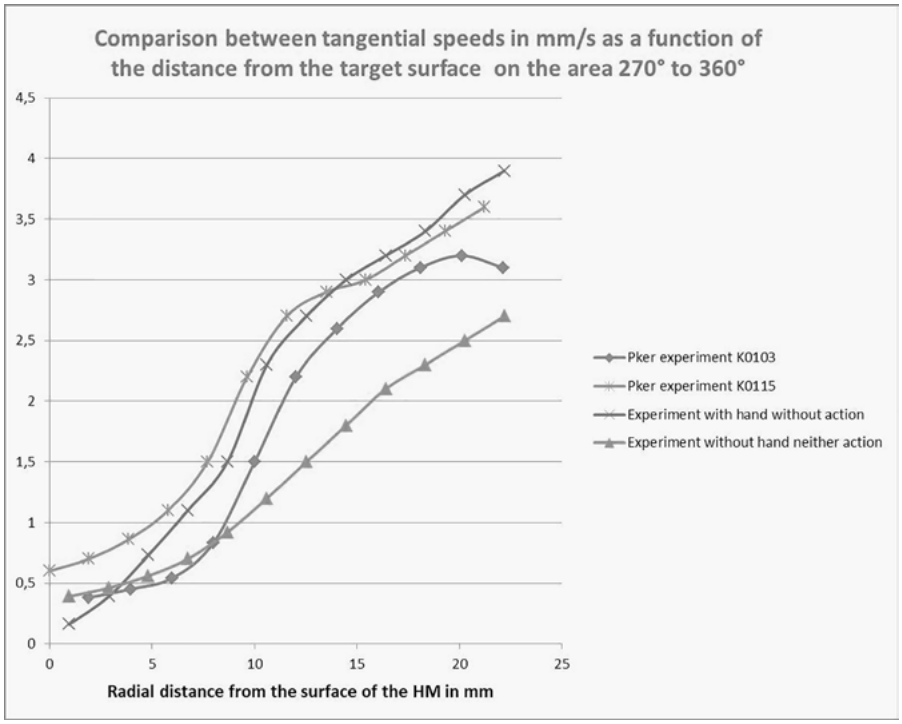

Figure R5. Tangential speeds in mm/s as a function of the radial distance from the HM surface in mm

With regard to the airflow speeds, there is no real difference between PKer experiments with action on the target and not. In the case where there is no hand in place, the speed of the airflow looks a bit lower beyond the 10 mm area zone. So, we can see an impact on the airflow because of the hand on

the top of the transportable bench, but it is small (on the order of 1 mm/s, which is far lower than the 20 mm/s required in the reference experiment).

Viewed from the perspective of reference experiments with the pump, there are no differences between these experiences, in terms of the airflow speeds. They are all producing very low speeds.

Conclusion

The reference experiments enable us to evaluate the minimal airflow speed required to set the HM target in motion (velocity between 23 and 31 mm/s, depending on the hose exit orientation) and the tangential speed at one centimeter from the surface of the HM (between 18.8 and 29.4 mm/s).

Compared to these, the experiments with the PKer yielded an airflow velocity as low as 2.4 mm/s (the other experiment at 2.7 mm/s) and the tangential speed at 1 cm from the surface of the HM as low as 1.5 mm/s (the other one at 2.2 mm/s). This gives a ratio for the tangential airflow speeds between the two kinds of experiments close to 10 (10.2 if we look at 1 cm from the surface of the HM).

This means that the target in the PKer experiment started to move with an airflow speed more than 10 times smaller than the required speed to start it (estimated in the reference experiment). Also, we saw in the PKer experiments that the hand on the top of the bench did not have a significant impact on the airflow speed (1 mm/s at most).

This confirms our hypothesis that the main cause that starts the HM motion in the PKer experiments, as presented, is not the airflow. As we have eliminated the other physical causes (see the subsection “Trickery detection / other causes for movement”), we appear to have demonstrated an Anomalous Perturbation, which could probably be attributed to some macro-PK effects.

Also, the experiments with this new portable PIV bench showed us that we are able to produce results with a good signal-to-noise ratio and with semi-repeatability (thanks to the PKer being able to set in motion three stacked MHs in this semi-confined environment). So, we invite other labs to try to reproduce this kind of experiment, in order to confirm these results.

Discussion

In Dullin and Jamet (2017b and 2018), several points associated with the methodological approach were discussed:

- the image acquisition error and frequency acquisition tolerance
- the calibration error
- the error induced by the PIV algorithm (image treatment)
- the difference between fluid and particle velocity.

The global error estimation for the final ratio presented was +/- 8.9%, so approximatively +/- 10%

which is minimal compared to the ratio of 1000% (factor 10) between the reference experiments airflow speed and the PKer experiments airflow speed. In addition, we would like to consider the following points:

- Vertical speed evaluation
- Global approach of slicing horizontally and vertically—Reynolds number justification
- Choice of impact zone for calculation

Finally, we will present a particular experiment with simulation of the heat generated by the hand and the upper body of the PKer.

Vertical PIV experiment for vertical speed evaluation

With the portable PIV bench, we are dealing with a semi-confined box with a rectangular opening at the top and burning incense sticks at the bottom to create the smoke. One could argue that this configuration could create an upward convection current reinforced by the heat of the PKer hand placed on the top of the box.

Even though our experiments showed no real impact of the hand placed at the top (maximum 1 mm/s increase in the airflow speed), this was on a horizontal plane, not on a vertical one. An upward current with disequilibrium around the HM could possibly induce a spin of the target. We did not have success in other experiments to produce a continuous movement of the HM by that means (even with only a single HM, whereas we have three stacked here), but we felt it was important to evaluate this scenario and conducted a new experiment with vertical PIV.

In order to measure the airflow speed in a vertical direction, the portable bench was used with the laser illuminating a vertical plane instead of a horizontal one, as in Figure D1.

Accordingly, the camera was set horizontally to record vertical images.

With this configuration, we performed a PKer experiment (K0054) with the three HMs stacked and made an analysis of the 10 seconds associated with the start of the target's motion. In Figure D2 we can see the results with the vector scale at 20. The mean velocity is 3.2 mm/s in the selected area.

So, these speeds are close to the ones we saw for the horizontal PIV.

On top of that, we recorded some videos without laser "slicing". So, we were able to see the flow of smoke all around the target and verify that we did not miss any particular event.

So, the speeds measured cannot explain the evolution of the target's motion (three HMs stacked), from stillness to a continuous spin, over the course of 4 minutes (with a final speed of 30 degrees/second).

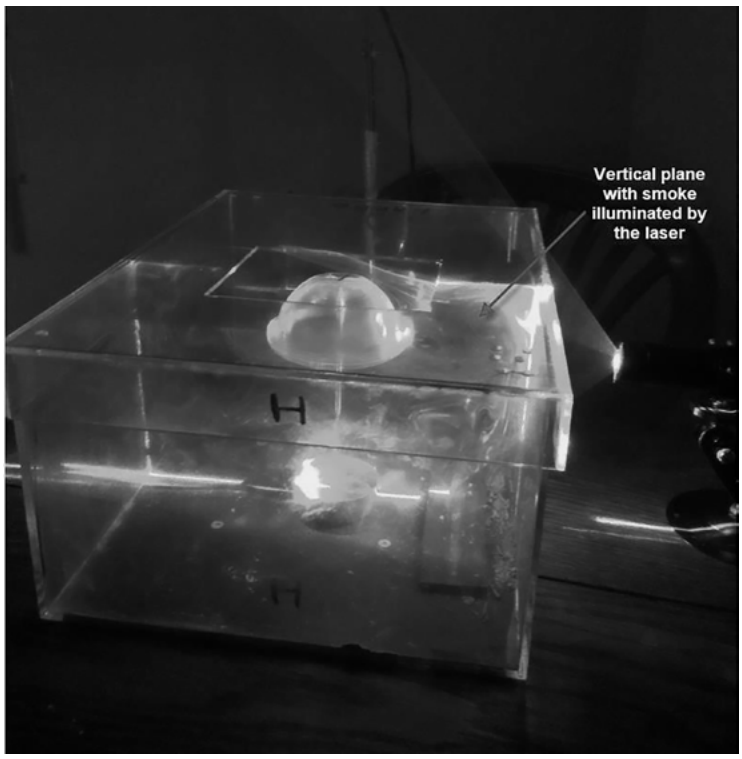

Figure D1. Vertical PIV configuration for the portable PIV bench

Figure D2. Vertical PIV—mean velocity magnitude in a selected area (vector scale 20)

Global approach of slicing horizontally and vertically—Reynolds number justification

In order to compare different experiments, we needed some reference criterion. The ultimate point of these experiences is to evaluate the role of the airflow around the target vis-à-vis its motion. The ideal situation would be to have a complete, three-dimensional view of the entire airflow around the HM and then compute the total torque applied by the airflow to the target over time. This is something really difficult to reach:

- The necessary set-up would be very complex to build, able to measure all the airflow speed in 3-D, in real time (50 images/s), even with the low speeds concerned.
- Even assuming all the data could be collected, it could be a hard task to transform this data into a torque value with good precision.

So, the way we approached it was to use reference experiments. First, we qualified the kind of flow concerned. So, we will use the Reynolds number, defined as

Re = ρ•V•D/μ, where ρ = density of the air, V = airflow speed, D = diameter of the HM and μ = dynamic viscosity of the air.

We are dealing with slow airflow speeds around the target (below 200 mm/s for the reference experiments and far below that for the PKer experiments).

For the range 200 mm/s to 10 mm/s, at ambient temperature (20 °C), Table 1 gives the Reynolds numbers, Re.

Table 1
Reynolds numbers (Re) for airflow speeds between 200 mm/s (0.200 m/s) and 10 mm/s (0.010 m/s)

Airflow speed (m/s)	0.200	0.100	0.050	0.025	0.010
Diameter (m)	0.073	0.073	0.073	0.073	0.073
Re	973.4	486.7	243.3	121.7	48.7

The Reynolds number for 200 mm/s is 973.4. So, we are clearly not in turbulent flow, for which the threshold often used is 2 400 (which would require, in our case, a speed of 500 mm/s). Because of that, what happens in one horizontal plane is similar to what happens in another horizontal plane (no shearing of the flow).

Then, in our reference experiment, we can work with an illuminated plane of smoke at the center part of the flow generated by the pump. It gives us a good approximation of the airflow field around the target. It is the same for the PKer experiments, and by using the same slice (at the same average height on the HM), we have a good basis for comparison between reference and PKer experiments. Also, the mean vertical speed study (see preceding paragraph) gave a confirmation of the airflow speed magnitude relative uniformity, with the vertical velocity magnitude being close to the horizontal velocity magnitude.

Choice of impact zone for calculation

There is a link between the mean airflow speed and the frictional torque around the mobile, which potentially drives it. In the reference experiment, the airflow is focused in a specific zone (determined by the direction of the hose exit). In this case, it is evident that the airflow speeds of concern for the triggering of the target spin are the ones in this specific zone. We can assume that the mean speed in this zone is greater than in any other zone around the target, on this horizontal plane.

In the reference experiments, we are trying to trigger the motion with a flow along the target; the main part of the flow impacts the bottom-left side of the HM (see Figure R1). If we look at the flows in the PKer experiments, they present speeds a bit higher in this zone, too. So, to avoid an arbitrary choice regarding the definition of the angular section on which to base the calculation of the representative mean tangential speed for each experiment, we decided to use the exact 270°–360° angular section (bottom-left part) of the HM for all experiments.

Then the resulting ratio of tangential speeds is a good approach to the comparison of the two kinds of experiments (this ratio could probably have been bigger if we had focused precisely on each higher speed zone in each experiment, but with the risk of many arbitrary choices).

Experiments with simulation of the heat generated by the hand and the upper body of the PKer

The objective here was to simulate the heat generated by the hand and the upper body of the PKer leaning on the bench and study if we could trigger a motion on the target.

We conducted different experiments, with three glasses filled with hot water (simulating the hand), another glass (simulating the wrist) and a big glass jar (simulating the upper body). Some of the glasses were filled with very hot water (90 °C, as in Figure D3), some with water at body temperature (37 °C at the glass surface). No motion of the target was observed at either temperature, as long as the PKer was not in the room.

In Figure D3, we can see the three glasses simulating the hand and the one simulating the wrist in their corresponding positions around the rectangular opening on the top of the bench. We can see also the glass jar representing the upper body of the PKer.

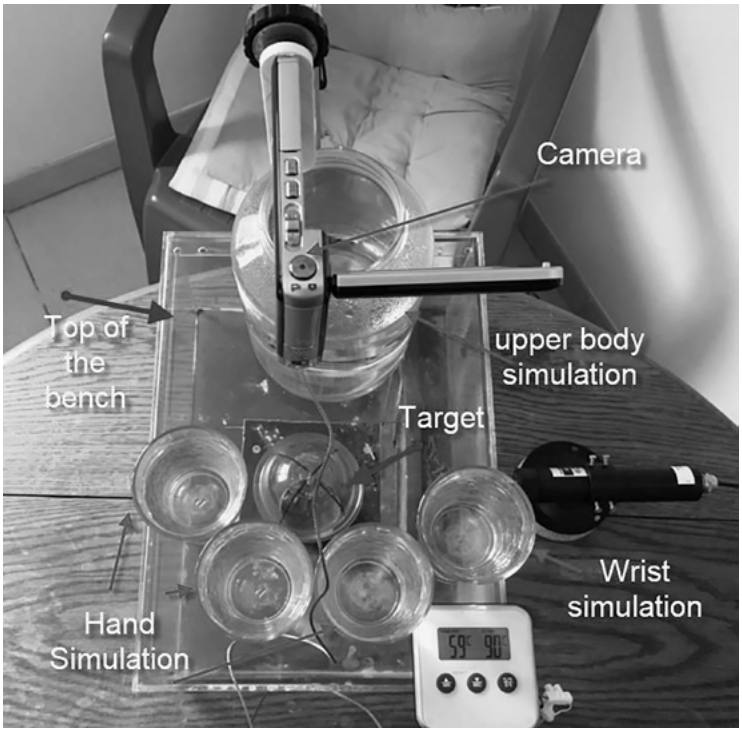

Figure D3. Simulation of hand, wrist and upper body with glasses and a glass jar filled with hot water

References

Black, C.M., & Carpenter, J.C. (2014, August 15). *A self-study of the role of mood on ostensible PK*. Paper presented at the 57th Annual Convention of the Parapsychological Association, Concord, CA.

Dullin, E. & Jamet, D. (2017a). Du moteur à fluide à la PK sur le net (From the bioforce motor to the PK on the Internet), *Métapsychique 1*, 76-85.

Dullin, E. & Jamet, D. (2017b, July 23). *Scientific evidence of telekinetic effects on a spinning mobile - A scientific attempt to detect and study telekinetic effects even in a non-confined environment*. Paper presented at the 60th Annual Convention of the Parapsychological Association, Athens.

Dullin, E. & Jamet, D. (2017c, September 3). *Telekinesis or aerodynamic/thermal effects?* Paper presented at the 41st International SPR Conference, London

Dullin, E. & Jamet, D. (2018). A methodology proposal for conducting macro-pk test on light spinning objects in a non-confined environment, *Journal of Scientific Exploration 32*: 514–554. doi: 10.31275/2018.1266.

Jahn, R. G., & Dunne, B. J. (2011). *Consciousness and the source of reality – The PEAR Odyssey.* ICRL Press

Puthoff, H. & Targ, R. (1974, August 26). *Physics, Entropy, and Psychokinesis*. Paper presented at Conference on quantum physics and parapsychology, Geneva

Roll, W. G. (1988, July 1). [Letter to Dr. Michael Glancey (University of Florida)]. William G. Roll papers (MS-0014, Box 170, Folder 44). Special collection Ingram library at University of West Georgia, Carrolton, GA

Un Banc Portable pour la Recherche sur les Effets Telékinétiques sur un Mobile Rotatif et les Résultats Expérimentaux Obtenus avec Lui

Résumé : Dans cet article, nous analysons précisément les conditions de départ du déplacement d'une cible rotative en nous focalisant sur les effets thermiques et aérodynamiques. Nous avons conduit des expérimentations de référence avec un banc statique, où le déplacement de l'objet est obtenu par le flux d'air issu d'une pompe, et des expérimentations avec un PKer (praticien volontaire de psychokinèse) avec un nouveau banc portable, dans laquelle le mouvement de la cible au sein du banc est déclenché par le Pker. La comparaison entre les vitesses de flux d'air tangentiels autour de la cible dans les deux configurations expérimentales a montré que les vitesses des flux d'air tangentiels dans les expérimentations avec PKer étaient dix fois plus faibles que les vitesses de flux d'air tangentiels requis pour démarrer le déplacement de la cible dans les expérimentations de référence. Les biais potentiels et les imprécisions de mesure et de calcul sont objectivement minimes comparés au facteur montré précédemment. Certains dispositifs expérimentaux spécifiques, simulant la main et le haut du corps du PKer à proximité du banc portable, ne provoquent aucune réaction de la cible. Ces différents éléments tendent à prouver que le déplacement de la cible dans ces expérimentations ne peut pas être attribué à des effets thermiques ou aérodynamiques. Le banc portable pourrait être un bon moyen pour que d'autres laboratoires tentent de reproduire et de confirmer ces expérimentations.

Eine tragbare Versuchsanordnung für die Untersuchung telekinetischer Effekte auf ein sich drehendes Mobile und die damit gewonnenen experimentellen Ergebnisse

Zusammenfassung: In diesem Beitrag analysieren wir präzise die Ausgangsbedingungen der Bewegung eines sich drehenden Targets unter besonderer Berücksichtigung der thermisch/aerodynamis-

chen Effekte. Wir führten Vergleichsexperimente mit einer feststehenden Versuchsanordnung durch, bei denen die Bewegung des Targets mit einer durch eine Pumpe erzeugten Luftströmung erzielt wird, und Experimente mit PKern (Freiwilligen, die Psychokinese praktizieren) (mit einer neuen tragbaren Versuchsanordnung), bei denen die Bewegung des Targets innerhalb der Versuchsanordnung durch die PKer ausgelöst wird. Der Vergleich zwischen den Strömungsgeschwindigkeiten der Luft um das Target in den beiden Versuchsgruppen zeigte, dass die tangentialen Strömungsgeschwindigkeiten der Luft in den Experimenten mit PKern 10mal niedriger waren, verglichen mit den tangentialen Strömungsgeschwindigkeiten der Luft, die notwendig waren, um das Target in den Vergleichsexperimenten in Bewegung zu setzen. Der potentielle Bias und die Fehler der Messung und Berechnung erweisen sich im Vergleich zu dem oben angegebenen Faktor als minimal. Einige spezielle Experimente, bei denen die Hand und der Oberkörper der PKer in der Nähe der tragbaren Versuchsanordnung simuliert wurden, lösten beim Target keine Reaktion aus. Diese verschiedenen Elemente deuten darauf hin, dass die Bewegung des Targets in diesen Experimenten nicht auf thermische/aerodynamische Effekte zurückzuführen ist. Die tragbare Versuchsanordnung könnte auch von anderen Laboratorien verwendet werden, um diese Experimente zu reproduzieren und zu bestätigen.

Un Banco Portátil para la Investigación de Efectos Telequinéticos en un Móvil Giratorio y los Resultados Experimentales Obtenidos con Él

Resumen. En este artículo analizamos precisamente las condiciones iniciales del movimiento de un objetivo giratorio enfocados en los efectos térmicos/aerodinámicos. Llevamos a cabo experimentos comparativos con un banco estático, donde el movimiento del objetivo se obtiene por el flujo de aire emitido por una bomba, y experimentos con un PK (un voluntario que practica psicoquinesis) (con un nuevo banco portátil), donde el movimiento del objetivo dentro del banco es activado por el PK. La comparación entre las velocidades de flujo de aire alrededor del objetivo en los dos grupos de experimentos mostró que las velocidades de flujo de aire tangencial en los experimentos PK fueron 10 veces más bajas que las velocidades de flujo de aire tangencial requeridas para iniciar el movimiento del objetivo en los experimentos de referencia. Mostramos que el sesgo y los errores potenciales en la medición y el cálculo son mínimos en comparación con el factor indicado anteriormente. Una configuración experimental, simulando la mano y la parte superior del cuerpo del PK cerca del banco portátil, no provocó ninguna reacción en el objetivo. Estos diferentes elementos tienden a demostrar que el movimiento del objetivo en estos experimentos no puede atribuirse a los efectos térmicos/aerodinámicos. El banco portátil puede ser una buena manera para que otros laboratorios intenten reproducir y confirmar estos experimentos.